AIP Journal of Applied Physics

Implantation-assisted Co-doped CdS thin films: Structural, optical, and vibrational properties

S. Chandramohan, A. Kanjilal, S. N. Sarangi, S. Majumder, R. Sathyamoorthy et al.

Citation: J. Appl. Phys. 106, 063506 (2009); doi: 10.1063/1.3224867
View online: http://dx.doi.org/10.1063/1.3224867
View Table of Contents: http://jap.aip.org/resource/1/JAPIAU/v106/i6
Published by the AIP Publishing LLC.

Additional information on J. Appl. Phys.

Journal Homepage: http://jap.aip.org/
Journal Information: http://jap.aip.org/about/about_the_journal
Top downloads: http://jap.aip.org/features/most_downloaded
Information for Authors: http://jap.aip.org/authors

ADVERTISEMENT

Running in Circles Looking for the Best Science Job?
Search hundreds of exciting new jobs each month!
http://careers.physicstoday.org/jobs
physicstoday JOBS

Downloaded 17 Sep 2013 to 136.167.3.36. This article is copyrighted as indicated in the abstract. Reuse of AIP content is subject to the terms at: http://jap.aip.org/about/rights_and_permissions

JOURNAL OF APPLIED PHYSICS **106**, 063506 (2009)

Implantation-assisted Co-doped CdS thin films: Structural, optical, and vibrational properties

S. Chandramohan,[1] A. Kanjilal,[2] S. N. Sarangi,[1] S. Majumder,[1] R. Sathyamoorthy,[3] and T. Som[1,a)]

[1]*Institute of Physics, Sachivalaya Marg, Bhubaneswar 751 005, India*
[2]*Institute of Ion Beam Physics and Materials Research, Forschungszentrum Dresden-Rossendorf, 01328 Dresden, Germany*
[3]*Department of Physics, Kongunadu Arts and Science College, Coimbatore 641 029, India*

(Received 8 July 2009; accepted 12 August 2009; published online 18 September 2009)

This paper reports on structural, optical, vibrational, and morphological properties of cobalt-doped CdS thin films, prepared by 90 keV Co^+ implantation at room temperature. In this work, we have used cobalt concentration in the range of 0.34–10.8 at. %. Cobalt doping does not lead to the formation of any secondary phase, either in the form of metallic clusters or impurity complexes. However, with increasing cobalt concentration a decrease in the optical band gap, from 2.39 to 2.26 eV, is observed. This reduction is addressed on the basis of band tailing due to the creation of localized energy states in association with Urbach energy calculations. In addition, implantation gives rise to grain growth and increase in the surface roughness. Size and shape fluctuations of individual CdS grains, at higher fluences, give rise to inhomogeneity in strain. The results are discussed in the light of ion-matter interaction in the keV regime. © *2009 American Institute of Physics*. [doi:10.1063/1.3224867]

I. INTRODUCTION

Cadmium sulfide (CdS) is one of the most technologically important group II-VI semiconductor due to its wide band gap [2.42 eV at room temperature (RT)], good photosensitivity, and easy tunable nonlinear optical properties.[1] Thin films and nanostructures of CdS are being widely investigated for their potential applications in various optoelectronic devices.[1,2] However, in order to achieve the desired properties and to make them multifunctional, a lot depends on doping CdS with different impurities. In this perspective, doping induced modifications in the structural, optical, electrical, and photoconduction properties of CdS thin films have been studied for various metal impurities such as Cu,[3] Al,[4] Sn,[5] etc. by several research groups. In recent years, transition metal (TM) (Mn, Fe, Co, etc.) doped CdS has drawn considerable attention as it offers a great opportunity to integrate electrical, optical, and magnetic properties into a single material, which makes it an ideal candidate for nonvolatile memory, magneto-optical, and future spintronic devices.[6–8] However, for any such application, a good understanding of doping induced changes in structural properties and its correlation with other physical properties is desirable.

Different techniques such as electrodeposition,[7] coevaporation,[9] chemical vapor deposition,[10] spray pyrolysis,[11] and other chemical routes[6] have been used to synthesize TM doped CdS. Ion implantation can also be considered as a viable technique for production of doped CdS thin films due to its many advantages over the conventional methods, viz., high spatial selectivity, precise control over maneuvering the impurity concentration, and possibility to overcome the solubility limit. Ion implantation is commonly used in microelectronics industry to achieve electrical isolation and selective area doping. It is known that solids subjected to ion bombardment experience creation of lattice disorder, which produces changes in structural, optical, and other physical properties of materials.[12,13] However, it also undergoes complex dynamic annealing process due to rapid collision cascades that depend on ion mass, energy, fluence, substrate temperature, etc. Thus, it is important to study implantation-assisted doping induced changes in physical properties, which would provide useful information to understand the performance of CdS based devices.

In this paper, in an attempt to synthesize Co-doped CdS thin films, we have made use of Co-ion implantation at RT and have studied changes in structural, optical, vibrational, and morphological properties for a wide range of dopant concentration. We have employed several complementary characterization techniques such as glancing angle x-ray diffraction (GAXRD), ultraviolet-visible-near-infrared (UV-visible-NIR) spectroscopy, atomic force microscopy (AFM), and micro-Raman spectroscopy. Our experimental data show that cobalt ion implantation (even at higher fluences) does not induce formation of any secondary phase or metallic clusters. Thus, CdS can be considered as a reasonably good radiation-resistant material. However, cobalt doping leads to modification in the optical band gap of CdS. In addition, we find that implantation at higher fluences gives rise to inhomogeneous strain due to fluctuations in size and shape of individual grains.

II. EXPERIMENTAL

CdS thin films (690 nm thick) were grown onto microglass slides at a substrate temperature of 373 K by thermal evaporation. Thickness and composition of the films were

a)Electronic mail: tsom@iopb.res.in.

 © 2009 American Institute of Physics

Downloaded 17 Sep 2013 to 136.167.3.36. This article is copyrighted as indicated in the abstract. Reuse of AIP content is subject to the terms at: http://jap.aip.org/about/rights_and_permissions

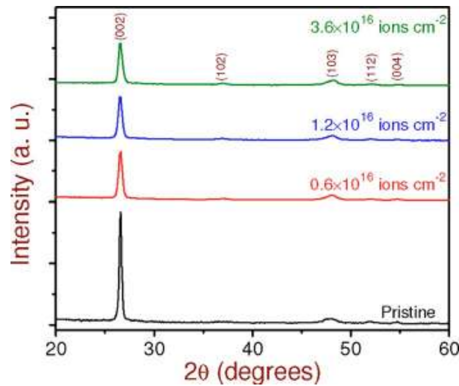

FIG. 1. (Color online) GAXRD patterns of the pristine and the Co^+-implanted CdS films for typical ion fluences of 0.6×10^{16}, 1.2×10^{16}, and 3.6×10^{16} ions cm^{-2}.

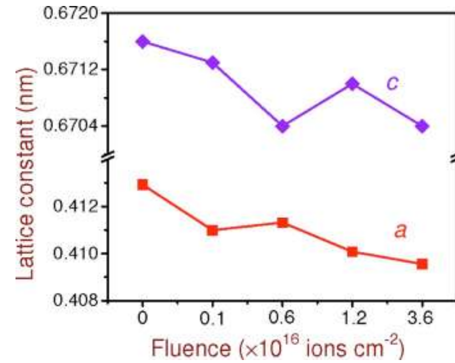

FIG. 2. (Color online) Variation in lattice constants [for the predominant (002) peak] as a function of ion fluence.

measured by Rutherford backscattering spectrometry. Subsequently, the films were uniformly implanted with 90 keV Co^+ ions at RT for a range of Co^+-ion fluences in the range of $0.1-3.6\times10^{16}$ ions cm^{-2}. These fluences correspond to the Co concentration of 0.34 to 10.8 at. % at the mean projected range. We used a target current of 2.5 μA distributed over an area of 4.5 cm^2 and the target holder was water cooled to avoid any temperature induced effect caused due to direct beam heating. Monte Carlo SRIM2008 simulation[14] predicts the projected range of 90 keV Co ions in CdS to be 58.7 nm with straggling of 29.7 nm.

Phase analysis of the pristine and the Co-doped CdS films was performed by GAXRD using the Cu-$K\alpha$ radiation ($\lambda=0.154$ nm). The optical absorption/transmittance measurements were carried out by using UV-visible-NIR spectrophotometer. Micro-Raman measurements were performed at RT in a backscattering geometry by using 532.14 nm line of neodymium-doped yttrium aluminum garnet laser excitation (green) with a power of 0.2 mW on the sample surface. The laser power was maintained at a lower value to avoid laser induced heating of the sample. AFM measurements were performed in the tapping mode. Images of all samples were collected from several regions.

III. RESULTS AND DISCUSSION

Figure 1 shows the GAXRD patterns recorded at a glancing angle $\theta_i=1°$ for the pristine and the samples implanted to different fluences. The pristine film is polycrystalline in nature and the observed peak positions match well with the hexagonal-close-packed, wurtzite structure of CdS with a preferential growth along the (002) direction.[15] It is observed that the polycrystalline nature of the pristine film is retained even after Co-ion implantation at the highest fluence. This indicates that CdS can be considered as a reasonably good radiation-resistant material. In addition, a decrease in the peak intensity takes place which could be due to cobalt doping induced high degree of damage produced during implantation. In addition, we observe a systematic increase in the full width at half maximum (FWHM) of the (002) peak with increasing ion fluence. Such an increase in the FWHM due to implantation-assisted doping have been reported for other systems as well.[12,16] According to the theory of kinematical scattering, FWHM of the XRD peaks are broadened either when crystallites become smaller or if lattice defects are present in large enough abundance.[17,18] We also do not observe formation of any metallic clusters or secondary phase precipitates unlike the results reported for ion implanted CdS.[13] This could happen due to the supersaturation of implanted ions occupying the substitutional cationic sites. Moreover, an overall decrease in the value of both *a*- and *c*-axis lattice constants was observed (as shown in Fig. 2). However, the lattice constants do not indicate a monotonous decrease but show changes between fluences of 0.6×10^{16} and 1.2×10^{16} ions cm^{-2}. The origin of such changes is not very clear to us but could be responsible due to irradiation induced multiple processes. These results are quite consistent with those reported for Co-doped[11,19] and Al-doped[4] CdS systems, prepared by conventional methods. In addition, Pandey *et al.*[20] also reported a similar kind of fluence dependent behavior of *c*-axis lattice constant for 200 keV Ni-ion implanted ZnO films. The observed lattice contraction implies that the incorporated Co atoms, having smaller ionic radii, are likely to occupy the substitutional cationic sites in the CdS lattice.

The band gap energy (E_g) of a direct band gap semiconductor like CdS can be estimated from the traditional Tauc plot of $(\alpha h\upsilon)^2$ versus photon energy ($h\upsilon$), as shown in Fig. 3. The band gap energy is obtained by extrapolating the linear part of the absorption curves to intercept the energy axis ($\alpha h\upsilon=0$). The inset in Fig. 3 depicts the variation in E_g with

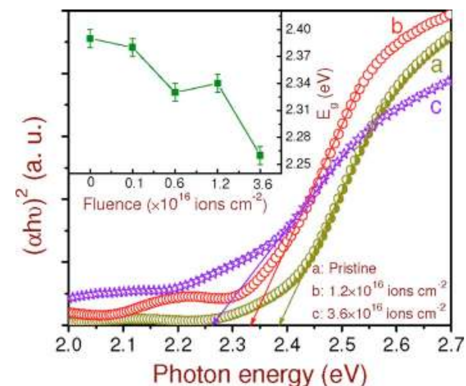

FIG. 3. (Color online) Plot of $(\alpha h\upsilon)^2$ vs $h\upsilon$ showing the estimation of direct band gap energy. The inset shows variation in the band gap (E_g) as a function of ion fluence.

Downloaded 17 Sep 2013 to 136.167.3.36. This article is copyrighted as indicated in the abstract. Reuse of AIP content is subject to the terms at: http://jap.aip.org/about/rights_and_permissions

ion fluence. The band gap of the pristine CdS film is found to be 2.39 eV, which decreases with increasing ion fluence (until 0.6×10^{16} ions cm^{-2}). Then it increases marginally at a fluence of 1.2×10^{16} ions cm^{-2} and thereafter sharply decreases to a value of 2.26 eV at the highest ion fluence (3.6×10^{16} ions cm^{-2}). Such changes in E_g between fluences of 0.6 and 1.2×10^{16} ions cm^{-2} are intrinsic and could be resulting from irradiation induced multiple processes. Band gap lowering due to the creation of either donor or acceptor states on doping CdS conventionally with impurity atoms like Cu, Sn, etc. is a known phenomenon.[3–5] However, modifications in the band gap caused by implantation induced doping can be mainly attributed to other effects such as defect-induced band tailing in semiconductors. In general, implanted ions are known to produce a large density of point defects (e.g., vacancies, interstitials, and antisite defects) causing lattice damage. For instance, SRIM2008 simulation predicts that the collision cascade of one single implanted Co ion creates about 21 vacancies nm^{-1} in CdS. These point defects can act as trap centers to affect the optical absorption. Therefore, a decrease in the optical band gap with increasing ion fluence could be primarily associated with defect-induced band tailing due to the creation of localized energy states near the band edges. Earlier studies on ion implanted CdS and CdSe thin films have demonstrated similar occurrence of band gap modification.[13,16,21] In addition, we observe a strong absorption below the band edge for the Co-doped samples, which is attributed to the transitions involving band tails.[22] The width of these band tail states can be described by the Urbach tail parameter or Urbach energy (E_U).[22] In our case, since the interference fringes overlap (for lower fluences), in order to justify the validity of change in the optical band gap due to implantation induced disorder, the Urbach energy is calculated for all fluences.

The optical absorption coefficient (α) just below the band edge in crystalline as well as disordered semiconductors involves transitions from or to localized states, and has an exponential-like dependence on photon energy. Such dependence of α, first observed by Urbach and later by Martienssen, is known as the Urbach–Martienssen or simply Urbach rule and is given by the following expression[23]

$$\alpha = \alpha_{\circ} \exp[\sigma(h\upsilon - E_{\circ})/kT], \quad (1)$$

where $\alpha_{\circ}$ and $E_{\circ}$ are characteristic parameters of the material, σ the steepness parameter, and T is the temperature. Equation (1) implies that a plot of $\ln(\alpha)$ against $h\upsilon$ near the band edge can be represented by a straight line, as shown in Fig. 4. The relation kT/σ, which is the width of the exponential tail, is called the Urbach energy, E_U. It generally represents the tailing of the valence-band density of states, which is broader than the conduction-band tail. In general, such an exponential absorption tail originates from the structural disorder, point defects, grain boundaries, compositional fluctuations, or inhomogeneous strain in thin films.[23–25] This is in good agreement with our GAXRD data described above. The estimated value of E_U for the Co-doped CdS films is plotted as a function of ion fluence (inset of Fig. 4). The value of E_U for the pristine CdS film is found to be 160 meV, which is comparable to the values reported for polycrystalline CdS

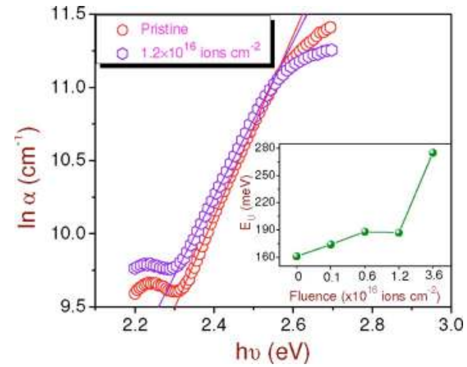

FIG. 4. (Color online) The logarithmic variation in absorption coefficient (α) with photon energy for the pristine and the Co-implanted sample to the fluence of 1.2×10^{16} ions cm^{-2}. The Urbach energy (E_U) is obtained from the slope of the liner fit (solid line) for the experimental data just below E_g. The inset depicts variation in E_U with Co-ion fluence.

films.[26,27] However, as the width of the tail depends on the degree of disorder, a unique value cannot be expected in case of thin films. We observe a systematic increase in E_U with increasing ion fluence (until 0.6×10^{16} ions cm^{-2}). Then it decreases marginally at a fluence of 1.2×10^{16} ions cm^{-2} and thereafter increases abruptly at the highest ion fluence (3.6×10^{16} ions cm^{-2}). Such an overall increase in E_U (but not monotonic) could result due to irradiation induced multiple processes, viz., cumulative structural disorder, creating more and more localized states within the band tails of the electronic states. In fact, a similar increase in E_U with increasing ion fluence is reported for Ar-ion implanted CdS films.[27] The latter could happen due to the production of high density of defects at higher ion fluence. It can be mentioned here that when the impurity concentration exceeds a certain limit, the highly doped impurity atoms can form an impurity band in the forbidden gap,[3] thus allowing a greater number of possible bands to have a tail in the forbidden energy region. This could be the possible reason for E_g to drop suddenly at the higher ion fluence (inset of Fig. 3). Moreover, the variations in the band gap energy and the Urbach energy show good correlation between each other. These results substantiate the expected interplay between the structural and the optical properties.

Raman scattering is a useful technique to examine the implantation induced lattice modification and disorder. Figure 5 shows the micro-Raman spectra of the pristine and the Co-implanted CdS films. The hexagonal wurtzite structured CdS belongs to the space group C^4_{6v}-$C6_3mc$ and at the center of the Brillouin zone, group theory predicts the following normal lattice vibrational modes:[28,29]

$$\Gamma_{\rm opt} = 1A_1 + 2B_1 + 1E_1 + 2E_2. \quad (2)$$

Among these, A_1, E_1, and E_2 are Raman active whereas B_1 is silent. For the A_1 branch the phonon polarization is in the z direction, whereas for the doubly degenerate E_1 and E_2 branches the phonon polarizations are in the xy plane. Because the wurtzite structure is noncentrosymmetric, both A_1 and E_1 modes split into longitudinal optical (LO) and transverse optical (TO) components by the macroscopic electric field associated with the longitudinal phonon. This electric

Downloaded 17 Sep 2013 to 136.167.3.36. This article is copyrighted as indicated in the abstract. Reuse of AIP content is subject to the terms at: http://jap.aip.org/about/rights_and_permissions

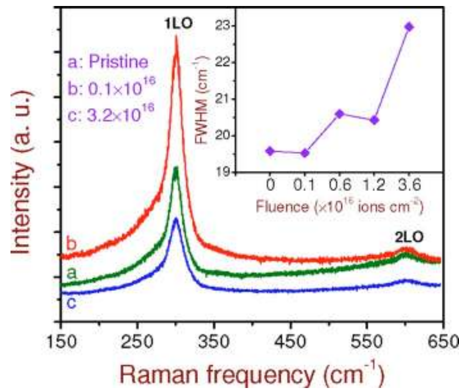

FIG. 5. (Color online) Raman spectra of the pristine and the Co^+-implanted CdS films for typical ion fluence of 0.1×10^{16} and 3.6×10^{16} ions cm^{-2}. The inset shows variation in the FWHM value of the 1 LO phonon line with ion fluence.

field serves to stiffen the force constant of the phonon and thereby raises the frequency of the LO over that of the TO. The Raman modes at about 300 and 601 cm^{-1} observed in the pristine sample (Fig. 5) correspond to the A_1 1LO and 2LO phonon modes, respectively.[4,29,30] The corresponding frequency of the 1LO mode in CdS crystals is reported to be 305 cm^{-1}.[4,27] Thus, we observe a downward peak shift of ~5 cm^{-1} for the pristine sample, which can be attributed to the grain-size effect or the surface phonon mode effect due to the small dispersion of LO phonon wave vector in polycrystalline films.[31] In our case, from the AFM studies, it is clear that the pristine films consist of small nanocrystalline grains (average size of 30 nm), which would be responsible for lowering the phonon frequencies.

Comparing the spectra of the pristine film and those of the implanted ones, we do not see any additional mode to get activated after Co-ion implantation. We observe an increase in the peak intensity and the peak area (under the 1LO Raman peak) with increasing ion fluence up to 1.2×10^{16} ions cm^{-2}. However, at the highest fluence (3.6×10^{16} ions cm^{-2}), the peak intensity drops to about 65% compared to that of the pristine sample. The increase in Raman peak intensity after implantation is in contrary to the usual situation that one would expect. In general, irradiation induced lattice disorder results in a decrease in the peak intensity and the peak area.[18] A similar kind of enhancement in the Raman peak intensity was reported for ion implanted CdS, CdSe, and ZnO samples at lower fluences and was attributed to the change in the surface roughness.[13,16,32] On the other hand, it is believed that the reduction in the peak intensity at the highest fluence could be dominated by disorder induced effects rather than the surface roughness. Further analysis of our micro-Raman data (shown in Fig. 5) reveal that for lower ion fluences (up to 0.6×10^{16} ions cm^{-2}) the 1LO peak position shifts toward a higher wavenumber and thereafter the amount of shift fluctuates (although the shifts are always toward higher wavenumbers compared to the pristine sample). Similar observations were reported for boron doped CdS thin films prepared by ion implantation.[33] Such optical phonon behaviors are related to strain and crystalline quality (which is influenced by lattice disorder).

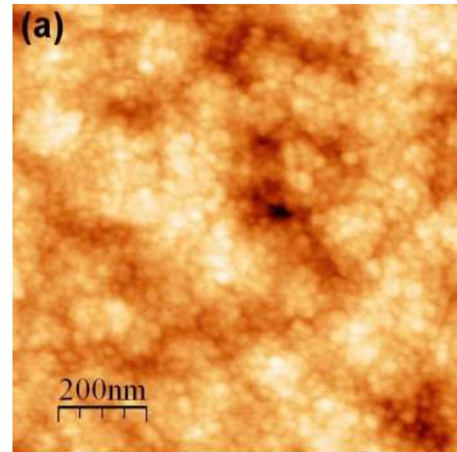

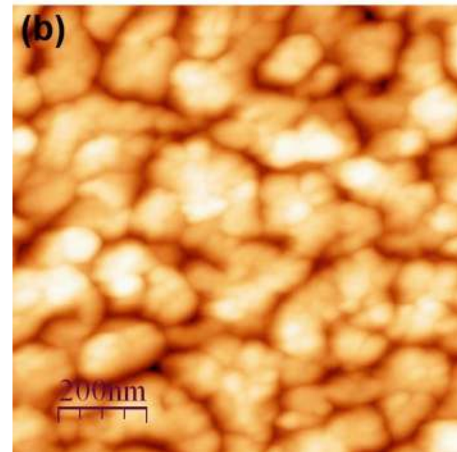

FIG. 6. (Color online) AFM images of CdS films: (a) pristine and (b) the sample implanted to the fluence of 1.2×10^{16} ions cm^{-2}.

The strain associated with a lattice contraction can be calculated using the following relation:

$$\Delta\omega/\omega_0 = (1+3\Delta c/c)^{-\gamma} - 1, \quad (3)$$

where $\Delta\omega$ is the 1LO phonon energy shift from its bulk value ω_0 (in our case it represents the pristine sample) and γ is the Grüneisen parameter (1.1 for CdS).[34,35] The calculated values show fluctuations at higher fluences which is quite consistent with our GAXRD measurements. From Fig. 5, we have also calculated the FWHM values of the 1LO peak and it is observed (inset of Fig. 5) that the peak gets broadened following Co-ion implantation. It may be mentioned that the FWHM value does not increase monotonously but shows fluctuation between the fluences of 0.6×10^{16} and 1.2×10^{16} ions cm^{-2} before it shows a sharp increase at the highest fluence. This anomaly in the variation in FWHM with ion fluence is intrinsic and could result from multiple processes governed by ion-matter interaction. The broadening of the phonon line shapes suggests an inhomogeneity in strain due to size and shape fluctuations of individual grains within the area that was sampled. This is quite consistent with our AFM measurements described below.

We have shown the representative AFM images in Fig. 6. Data analysis shows a systematic increase in the root-mean-square surface roughness (R_q) with increasing ion flu-

Downloaded 17 Sep 2013 to 136.167.3.36. This article is copyrighted as indicated in the abstract. Reuse of AIP content is subject to the terms at: http://jap.aip.org/about/rights_and_permissions

ence. For instance, the measured value of R_q for the pristine sample is 3.8 nm which increases up to 15.4 nm for the highest fluence. The rough surface results from the damage caused by implantation induced doping at high fluences. In addition, it is clear from the morphology of the pristine and the doped films that due to cobalt implantation at higher fluences, the boundary among the smaller grains slowly smear out and large moundlike structures of different dimensions and shapes grow. Implantation induced grain growth has been reported for other systems as well.[20] These observations corroborate well with our other measurements described above.

Let us now discuss our results in the light of ion-solid interaction. Interaction of ions with matter in the energy range under consideration is dominated by nuclear energy loss caused by elastic collision between incident ions and target atoms. As a result, a dense collision cascade gets developed in a solid when energetic ions travel through it. Time evolution of such a collision cascade can be divided into different phases.[36] The initial stage, during which atoms collide strongly, is known as the collisional phase and has a lifetime of $\sim 0.1-1$ ps. Due to such collisional events all atoms near the ion path are set into thermal motion at a high temperature. This high temperature spreads and reduces within the lattice by heat conduction. This is known as thermal spike phase and it lasts for ~ 1 ns. As a result, a large number of defects are created in the solid. These defects can be of several types, viz., vacancies, interstitial atoms, complex interstitial-dislocation loops, and volume defects.[37,38] Based on the electron bombardment experiments performed with 100–300 keV electrons, it has been reported by Kulp[39] that the threshold energy required to knock out the Cd and the S atoms from their lattice positions is 7.3 and 8.7 eV, respectively. Thus, it is easier to displace a Cd atom than an S atom in the CdS lattice. Moreover, the binding energy of Cd atoms is smaller than that of S atoms.[5] As a result implanted Co atoms can displace Cd atoms to the interstitial positions and occupy the resultant vacancies. This fits well with our results described above.

IV. SUMMARY AND CONCLUSIONS

In summary, we have studied structural, optical, vibrational, and morphological properties of Co-doped CdS thin films (from 0.34 to 10.8 at. %) prepared by ion implantation at RT. We do not observe formation of any secondary phase or metallic clustering, which shows the efficacy of this technique for synthesis of Co-doped CdS thin films. In addition, we observe that the implanted Co atoms occupy the substitutional cationic sites in the CdS lattice. Co-doping at RT causes modification in the optical band gap of CdS by creating localized energy states near the band edges. Implantation creates grain growth, enhanced roughness, and a large degree of disorder at higher fluences. In addition, implantation causes strain in the CdS lattice which is inhomogeneous at higher fluences due to size and shape fluctuations of individual grains. The present investigation provides a wealth of information, which would be useful for further development of CdS based devices.

ACKNOWLEDGMENTS

We acknowledge F. Ludewig for his help in ion implantation. Thanks are due to S. Varma and S. N. Sahu for their help regarding the AFM, optical, and vibrational studies.

[1]N. V. Hullavarad, S. S. Hullavarad, and P. C. Karulkar, J. Nanosci. Nanotechnol. **8**, 3272 (2008).
[2]J. B. Seon, S. Lee, J. M. Kim, and H. D. Jeong, Chem. Mater. **21**, 604 (2009).
[3]P. J. Sebastian, Appl. Phys. Lett. **62**, 2956 (1993).
[4]H. Khallaf, G. Chai, O. Lupan, L. Chow, S. Park, and A. Schulte, J. Phys. D **41**, 185304 (2008).
[5]P. Roy and S. K. Srivastava, J. Phys. D **39**, 4771 (2006).
[6]J. S. Kulkarni, O. Kazakova, and J. D. Holmes, Appl. Phys. A: Mater. Sci. Process. **85**, 277 (2006).
[7]J. C. Lee, N. G. Subramaniam, J. W. Lee, and T. W. Kang, Appl. Phys. Lett. **90**, 262909 (2007).
[8]E. Oh, J. H. Choi, D. K. Oh, and J. Park, Appl. Phys. Lett. **93**, 041911 (2008).
[9]D. H. Kim, D. J. Lee, N. M. Kim, S. J. Lee, T. W. Kang, Y. D. Woo, and D. J. Fu, J. Appl. Phys. **101**, 094111 (2007).
[10]K. W. Liu, J. Y. Zhang, D. Z. Shen, X. J. Wu, B. H. Li, B. S. Li, Y. M. Lu, and X. W. Fan, Appl. Phys. Lett. **90**, 092507 (2007).
[11]E. Bacaksiz, M. Tomakin, M. Altunbas, M. Parlak, and T. Colakoglu, Physica B **403**, 3740 (2008).
[12]A. Mendoza-Galván, C. Trejo-Cruz, J. Lee, D. Bhattacharyya, J. Metson, P. J. Evans, and U. Pal, J. Appl. Phys. **99**, 014306 (2006).
[13]K. Senthil, D. Mangalaraj, Sa. K. Narayandass, B. Hong, Y. Roh, C. S. Park, and J. Yi, Semicond. Sci. Technol. **17**, 97 (2002).
[14]J. F. Zeigler, J. P. Biersack, and U. Littmark, *The Stopping and Ranges of Ions in Solids* (Pergamon, New York, 1985), Vol. 1 (http://www.srim.org/).
[15]JCPDS—International Centre for Diffraction Data, Powder Diffraction File No. 77-2306 (ICDD, Newton Square, PA, 1997).
[16]S. Venkatachalam, D. Mangalaraj, Sa. K. Narayandass, R. Kesavamoorthy, P. Magudapathy, B. Sundaravel, S. Kalavathi, and K. G. M. Nair, Semicond. Sci. Technol. **21**, 1661 (2006).
[17]T. Ungar, Scr. Mater. **51**, 777 (2004).
[18]R. Sivakumar, C. Sanjeeviraja, M. Jayachandran, R. Gopalakrishnan, S. N. Sarangi, D. Paramanik, and T. Som, J. Phys.: Condens. Matter **19**, 186204 (2007).
[19]K. A. Bogle, S. Ghosh, S. D. Dhole, V. N. Bhoraskar, L.-f. Fu, M. Chi, N. D. Browning, D. Kundaliya, G. P. Das, and S. B. Ogale, Chem. Mater. **20**, 440 (2008).
[20]B. Pandey, S. Ghosh, P. Srivastava, P. Kumar, and D. Kanjilal, J. Appl. Phys. **105**, 033909 (2009).
[21]S. Chandramohan, A. Kanjilal, J. K. Tripathi, S. N. Sarangi, R. Sathyamoorthy, and T. Som, J. Appl. Phys. **105**, 123507 (2009).
[22]B. Han, B. W. Wessels, and M. P. Ulmer, J. Appl. Phys. **98**, 023513 (2005).
[23]S. M. Wasim, C. Rincon, G. Marın, P. Bocaranda, E. Hernandez, I. Bonalde, and E. Medina, Phys. Rev. B **64**, 195101 (2001).
[24]Z. G. Hu, W. W. Li, J. D. Wu, J. Sun, Q. W. Shu, X. X. Zhong, Z. Q. Zhu, and J. H. Chu, Appl. Phys. Lett. **93**, 181910 (2008).
[25]A. Cremades, L. Gorgens, O. Ambacher, and M. Stutzmann, Phys. Rev. B **61**, 2812 (2000).
[26]A. E. Rakhshani, J. Phys.: Condens. Matter **12**, 4391 (2000).
[27]K. L. Narayanan, K. P. Vijayakumar, K. G. M. Nair, and N. S. Thampi, Physica B **240**, 8 (1997).
[28]C. A. Arguello, D. L. Rousseau, and S. P. S. Porto, Phys. Rev. **181**, 1351 (1969).
[29]H. Pan, G. Xing, Z. Ni, W. Ji, Y. P. Feng, Z. Tang, D. H. C. Chua, J. Lin, and Z. Shen, Appl. Phys. Lett. **91**, 193105 (2007).
[30]K.-Y. Lee, J.-R. Lim, H. Rho, Y.-J. Choi, K. J. Choi, and J.-G. Park, Appl. Phys. Lett. **91**, 201901 (2007).
[31]D. S. Chuu and C. M. Dai, Phys. Rev. B **45**, 11805 (1992).
[32]J. D. Ye, S. Tripathy, F.-F. Ren, X. W. Sun, G. Q. Lo, and K. L. Teo, Appl. Phys. Lett. **94**, 011913 (2009).
[33]K. L. Narayanan, M. Yamaguchi, J. A. Davila-Pintle, R. Lozada-Morales, O. Portillo-Moreno, and O. Zelaya-Angel, Vacuum **81**, 1430 (2007).

Downloaded 17 Sep 2013 to 136.167.3.36. This article is copyrighted as indicated in the abstract. Reuse of AIP content is subject to the terms at: http://jap.aip.org/about/rights_and_permissions

[34]J.-Y. Zhang, X.-Y. Wang, M. Xiao, L. Qu, and X. Peng, Appl. Phys. Lett. **81**, 2076 (2002).
[35]G. Scamarcio, M. Lugará, and D. Manno, Phys. Rev. B **45**, 13792 (1992).
[36]W. Bolse, Mater. Sci. Eng. R. **12**, 53 (1994).
[37]K. Saarinen, P. Hautojärvi, J. Keionen, E. Rauhala, J. Räisänen, and C. Corbel, Phys. Rev. B **43**, 4249 (1991).
[38]T. Diaz de la Rubia and M. W. Guinan, Phys. Rev. Lett. **66**, 2766 (1991).
[39]B. A. Kulp, Phys. Rev. **125**, 1865 (1962).

Downloaded 17 Sep 2013 to 136.167.3.36. This article is copyrighted as indicated in the abstract. Reuse of AIP content is subject to the terms at: http://jap.aip.org/about/rights_and_permissions